

Towards a standard gamma-ray burst: tight correlations between the prompt and the afterglow plateau phase emission

M. G. Dainotti,^{1*} M. Ostrowski^{1*} and R. Willingale^{2*}

¹*Observatorium Astronomiczne, Uniwersytet Jagiellonski, ul. Orla 171, 31-501 Krakow, Poland*

²*Department of Physics and Astronomy, University of Leicester, University Road, Leicester LE1 7RH*

Accepted 2011 July 13. Received 2011 July 13; in original form 2011 April 6

ABSTRACT

To find out the astrophysical processes responsible for gamma-ray burst (GRB), it is crucial to discover and understand the relations between their observational properties. This work was performed in the GRB rest frames using a sample of 62 long *Swift* GRBs with known redshifts. Following the earlier analysis of the correlation between afterglow luminosity (L_a^*) and break time (T_a^*), we extend it to correlations between the afterglow and the prompt emission GRB physical parameters. We find a tight physical scaling between the mentioned afterglow luminosity L_a^* and the prompt emission mean luminosity $\langle L_p^* \rangle_{45} \equiv E_{\text{iso}}/T_{45}^*$. The distribution, with the Spearman correlation coefficient reaching 0.95 for the most accurately fitted subsample, scales approximately as $L_a^* \propto \langle L_p^* \rangle_{45}^{0.7}$. We have also analysed correlations of L_a^* with several prompt emission parameters, including the isotropic energy E_{iso} and the peak energy in the νF_ν spectrum, E_{peak} . As a result, we obtain significant correlations also between these quantities, discovering that the highest correlated GRB subsample in the afterglow analysis leads also to the highest prompt–afterglow correlations. Such events can be considered to form a sample of standard GRBs for astrophysics and cosmology.

Key words: radiation mechanisms: non-thermal – gamma-ray burst: general.

1 INTRODUCTION

To better understand the processes responsible for gamma-ray bursts (GRBs) and possibly to create a new GRB-based cosmological standard candle, one should find out the universal properties by looking for strict relations among their observables. But, GRBs seem to be everything but standard candles, with their energetics spanning over 8 orders of magnitude. However, the reported correlations of $E_{\text{iso}}-E_{\text{peak}}$ (Lloyd & Petrosian 1999; Amati et al. 2002; Amati, Frontera & Guidorzi 2009), $E_\gamma-E_{\text{peak}}$ (Ghirlanda, Ghisellini & Lazzati 2004; Ghirlanda, Ghisellini & Firmani 2006), $L-E_{\text{peak}}$ (Schaefer 2003; Yonekoto 2004), $L-V$ (Fenimore & Ramirez-Ruiz 2000; Riechart et al. 2001) and other proposed luminosity indicators (Norris, Marani & Bonnell 2000; Liang & Zhang 2005, 2006) raised the expectation of a quick progress in the field. The problem of large data scatter in the considered luminosity relations (Butler, Kocevski & Bloom 2009; Yu, Qi & Lu 2009) and a possible impact of detector thresholds on cosmological standard candles (Shahmoradi & Nemiroff 2009) are also debated issues (Cabrera et al. 2007). The underlying problem of the scatter in all the correlations is that it is larger than the spread

expected of the z dependence alone. GRBs can be seen from a large fraction of the visible Universe, up to $z = 9.4$ (Cucchiara et al. 2011). The luminosity spread due to, exclusively, its luminosity distance squared dependence gives for the limiting redshifts a factor of $D_L^2(9.4)/D_L^2(0.085) = 6.4 \times 10^4$ while the actual spread in luminosity is 8 orders of magnitude $10^{46}-10^{54}$ erg s⁻¹. It is not clear what is responsible for such a large dynamic range.

Among various attempts, Dainotti, Cardone & Capozziello (2008) have proposed a way to standardize GRBs with the discovery of $\log L_a^* - \log T_a^*$ (LT) anticorrelation, where $L_a^* \equiv L_X^*(T_a)$ is an isotropic X-ray luminosity in the time T_a^* , the transition time separating the plateau and the power-law decay afterglow phases and, henceforth, we use the index ‘*’ to indicate quantities measured in the GRB rest frame.¹ We have presented (Dainotti et al. 2010) an analysis revealing that the long GRBs with smaller values of the error parameters in the afterglow are much more tightly LT correlated as compared to the full sample of long GRBs. The LT correlation has been already applied to derive cosmological parameters (Cardone, Capozziello & Dainotti 2009; Cardone et al. 2010). Moreover, one may note that an analogous LT relation was derived phenomenologically (Ghisellini et al. 2009; Yamazaki 2009) and

*E-mail: dainotti@oa.uj.edu.pl (MGD); mio@oa.uj.edu.pl (MO); rw@star.le.ac.uk (RW)

¹ Note a change of notation with respect to our previous papers, where we used the symbol L_X^* – without an index ‘a’ – to indicate $L_X^*(T_a^*)$.

Table 1. A data list for GRBs with known redshifts analysed in this paper: 62 long GRBs with $u < 4$ (upper part of the table) and 11 IC GRBs (lower part of the table). The U0.095 subsample is indicated by ash attached to their u values. The full version of this table is present at <http://www.mpe.mpg.de/~jcg/grb.html>.

IdGRB	z	β_{ta_a}	$F \times x$ ($\text{erg cm}^{-2} \times s$)	$\log T_{90}^*$ (s)	$\log T_{45}^*$ (s)	$\log T_p^*$ (s)	$\log L_a^*$ (s)	$\log L_a^*$ (erg s^{-1})	$\log E_{\text{iso}}$ (erg)
050315	1.95	0.89 ± 0.04	$4.58\text{E-}12 \pm 1.97\text{E-}12$	1.510 ± 0.014	0.816 ± 0.018	1.010 ± 0.037	3.92 ± 0.17	46.19 ± 0.19	52.75 ± 0.14
050318	1.44	0.93 ± 0.18	$1.00\text{E-}08 \pm 1.41\text{E-}08$	1.100 ± 0.001	0.157 ± 0.024	-1.770 ± 0.132	1.62 ± 0.59	49.35 ± 0.62	52.08 ± 0.04
050319	3.24	0.85 ± 0.02	$4.31\text{E-}12 \pm 1.78\text{E-}12$	1.560 ± 0.005	0.452 ± 0.032	0.260 ± 0.099	4.04 ± 0.16	46.43 ± 0.18	52.66 ± 0.20
050401	2.9	1.00 ± 0.04	$3.87\text{E-}11 \pm 1.33\text{E-}11$	0.945 ± 0.006	0.125 ± 0.033	-1.480 ± 0.316	3.28 ± 0.14	47.24 ± 0.15	53.51 ± 0.13
050416A	0.65	0.99 ± 0.10	$1.06\text{E-}11 \pm 5.62\text{E-}12$	0.245 ± 0.044	-0.418 ± 0.041	0.042 ± 0.105	2.97 ± 0.21	45.83 ± 0.23	51.00 ± 0.09
050505	4.26	1.09 ± 0.04	$4.93\text{E-}12 \pm 3.84\text{E-}12$	1.060 ± 0.007	0.260 ± 0.036	0.137 ± 0.882	3.67 ± 0.33	46.42 ± 0.34	53.20 ± 0.13
050603	2.82	0.91 ± 0.10	$1.10\text{E-}12 \pm 6.64\text{E-}13$	0.409 ± 0.026	-0.378 ± 0.027	-0.230 ± 0.199	4.25 ± 0.25	45.74 ± 0.27	53.70 ± 0.16
050730	3.97	0.52 ± 0.27	$6.59\text{E-}11 \pm 1.12\text{E-}11$	1.080 ± 0.021	0.626 ± 0.021	0.695 ± 0.052	3.44 ± 0.04	47.92 ± 0.20	52.95 ± 0.16
050801	1.56	1.43 ± 0.30	$4.23\text{E-}11 \pm 1.62\text{E-}11$	0.363 ± 0.036	-0.408 ± 0.043	0.690 ± 0.197	2.17 ± 0.15	46.76 ± 0.18	51.54 ± 0.21

it is also a useful test for the models (Cannizzo & Gehrels 2009; Cannizzo, Troja & Gehrels 2011; Dall’Osso et al. 2011).

GRBs have been traditionally classified as *short/hard* ($T_{90} < 2$ s) and *long/soft* ($T_{90} > 2$ s), where T_{90} usually denotes the time duration of the GRB (Kouveliotou et al. 1993). However, the existence of an intermediate GRB class (IC), as an apparent (sub)class of bursts with a short initial pulse followed by an extended low-intensity emission phase has been revealed (Norris & Bonnell 2006). It requires a revision of the above simple scheme. In our analysis we consider only long GRBs, but on some plots with GRB distributions we also show the IC class events demonstrating remarkable differences as compared to the long bursts.

Here we study correlations between the *afterglow* luminosity parameter L_a^* and the energetics and mean luminosity of the *prompt emission*. We demonstrate the existence of significant correlations among the afterglow plateau and the prompt emission phases, which reach a maximum for the *Swift* light curve well fitted by a simple analytical expression proposed by Willingale et al. (2007). The obtained high correlations indicate the expected physical coupling between the GRB prompt and afterglow energetics, which is quite tight for the well-fitted afterglow light-curve GRBs [called in Dainotti et al. (2010) the *upper envelope*]. We also find that the prompt–afterglow correlations are more significant if one uses the prompt emission mean luminosity instead of the energy E_{iso} . This work reveals an important fact: any search for physical relations between GRB properties should involve selection of well-constrained physical GRB subsamples. Use of all the available data introduces into the analysis events with highly scattered intrinsic physical properties, which serves to smooth out possible correlations, and may lead to systematic shifts in the fitted relations; see Dainotti et al. (2010). It is likely that a substantial fraction of the observed large scatter is introduced because we are observing different classes of GRBs with different progenitors and/or in different physical conditions. Identifying such subclasses may be the real challenge. Separating short and long GRBs is too simplistic. In this paper we use CGS units: erg for energy, erg s^{-1} for luminosity and s for time. All the quantities used for correlation analysis are computed in the GRB rest frames (we indicate such quantities using a superscript *, E_{iso} is in GRB rest frame from its definition).

2 DATA SELECTION AND ANALYSIS

We can estimate the characteristic luminosity of a burst using different characteristic times, T_{45} , T_{90} and T_p , where T_{90} is the time interval during which the background-subtracted cumulative counts increase from 5 to 95 per cent (Kouveliotou et al. 1993), T_{45} is the

time spanned by the brightest 45 per cent of the total counts above the background (Riechart et al. 2001) and T_p is the fitted transition time in which the exponential decay in the prompt phase changes to a power-law decay (Willingale et al. 2007). Here we define $\langle L_p^* \rangle_{45} \equiv E_{\text{iso}}/T_{45}^*$, $\langle L_p^* \rangle_{90} \equiv E_{\text{iso}}/T_{90}^*$ and $\langle L_p^* \rangle_{T_p} \equiv E_{\text{iso}}/T_p^*$ and analyse correlations between logarithms of the prompt emission parameters E_{iso} , $\langle L_p^* \rangle_{45}$, $\langle L_p^* \rangle_{90}$, $\langle L_p^* \rangle_{T_p}$, E_{peak} , V and the parameters L_a^* and T_a^* characterizing the afterglow light curve.

The GRB sample used in the analysis is composed of all afterglows with known redshifts detected by *Swift* from 2005 January up to 2009 April (Dainotti et al. 2010), with the light curves possessing the early X-ray telescope (XRT) data, enabling fitting by the Willingale et al. (2007) phenomenological model. The redshifts z are taken from the Greiner’s web site <http://www.mpe.mpg.de/~jcg/grb.html>. We have compared these redshifts with the values reported in literature (Butler et al. 2007; Butler, Bloom & Poznanski 2009) and we find that they agree well apart from two cases of GRB 050801 and 060814, but Butler (private communication) suggested that we should use the Greiner redshifts for those two cases. The E_{iso} , E_{peak} , T_{90} and T_{45} and V values are listed in literature (Butler et al. 2007, 2009; Xiao & Schaefer 2009). The fitted values of T_p used for the determination of L_a^* (Dainotti et al. 2010) are given in the on-line data Table 1 at <http://www.oa.uj.edu.pl/M.Dainotti/GRB2011>. Derivations of T_a^* and L_a^* for each afterglow follow Dainotti et al. (2010) and Willingale et al. (2007):

$$L_a^* = \frac{4\pi D_L^2(z) F_X(T_a)}{(1+z)^{1-\beta_a}}, \quad (1)$$

where β_a is the X-ray spectral index of the emission at T_a , $F_X(t)$ is the fitted flux computed at the time $t = T_a$ and $D_L(z)$ is the source luminosity distance. We have computed the luminosities assuming that the spectrum could be fitted with a simple power law (Evans et al. 2009; Dainotti et al. 2010). For $D_L(z)$ we have adopted a flat Friedman–Robertson–Walker cosmological model with $H_0 = 71 \text{ km s}^{-1} \text{ Mpc}^{-1}$ and $\Omega_m = 0.3$ [see the online Table 1 at <http://www.oa.uj.edu.pl/M.Dainotti/GRB2011>, contrary to Dainotti et al. (2010), where slightly different values were used].

Below, the fitted power-law relation between the analysed quantities ‘ X ’ and ‘ Y ’ is $\log X = \log b + a \times \log Y$ on the logarithmic plane, where the constants a and b are determined using the D’Agostini method (D’Agostini 2005).

Our full analysed sample of 77 GRBs with the redshift range of 0.08–8.26 includes 66 long GRBs afterglows and 11 GRBs whose nature is debated, the claimed intermediate class (IC) between long and short GRBs. Our long-GRB sample also includes eight X-Ray flashes (XRFs) [060108, 051016B, 050315, 050319 (Gendre, Galli & Piro 2007); 050401, 050416A, 060512, 080330

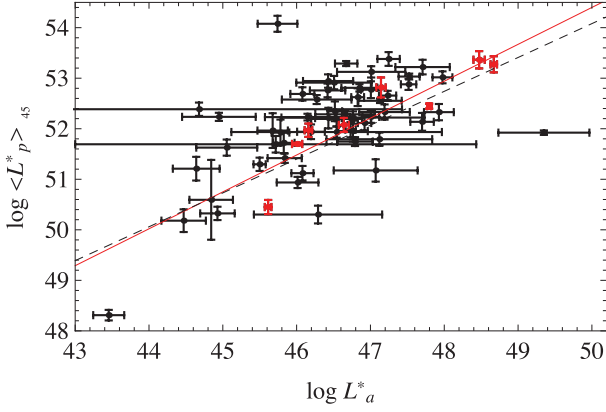


Figure 1. L_a^* versus $\langle L_p^* \rangle_{45}$ distribution for the U4 sample (all points), with black dashed line showing the fitted correlation. The red line is fitted to the eight lowest error (red) points of the U0.095 subsample.

(Sakamoto 2008)]. To constrain the study to physically homogeneous samples, we have analysed the subsamples of 66 long GRBs (including XRFs) and of 11 IC ones separately, following the approach adopted in Dainotti et al. (2010). From a homogeneous sample of long GRBs we extract subsamples of GRBs with improving Willingale’s light-curve fit quality.

As a measure of the fit accuracy (L_a^* , T_a^*) we use the error parameter u :

$$u \equiv \sqrt{\sigma_{L_a^*}^2 + \sigma_{T_a^*}^2} \quad (2)$$

as defined in Dainotti et al. (2010). One note that it is also a relative error in measuring the X-ray energy scale $L_a^* \times T_a^*$. The error parameter u is determined by several factors, such as the errors of the individual data points and their number, but particularly by its distribution near the break time T_a . This error parameter is a better discriminator for the LT correlation than chi square, because the latter depends on the errors and the number of data points of all the light curves.

In this study the limiting long-GRB subsamples are the following: the largest one consisting of 62 long GRBs with $u \leq 4$, hereafter called ‘U4’; and the subsample that was previously called the *upper envelope*, consisting of eight GRBs with the smallest afterglow fit errors, $u \leq 0.095$, hereafter called ‘U0.095’. We also analyse selected intermediate subsamples with the maximum u values decreasing from 4.0 to 0.095, in attempt to reveal systematic variations in the studied correlations. This choice follows our previous paper, Dainotti et al. (2010), and the discussion of the systematics issues has been already presented in Dainotti et al. (2011).

3 PROMPT-AFTERGLOW CORRELATIONS

The derived $\log L_a^* - \log \langle L_p^* \rangle_{45}$ distribution is presented for the U4 subsample of 62 long GRBs in Fig. 1, where the U0.095 subsample of eight GRBs with the most accurate determination of L_a^* and T_a is also indicated. The distribution illustrates a significant correlation of the considered luminosities, with the Spearman correlation coefficient,² ρ , equal to 0.64 for U4 but growing to 0.98 for U0.095 sample (Fig. 1). The fitted distribution reads $\log L_a^* \propto \log \langle L_p^* \rangle_{45}^a$,

² A non-parametric measure of statistical dependence between two variables (Spearman 1904).

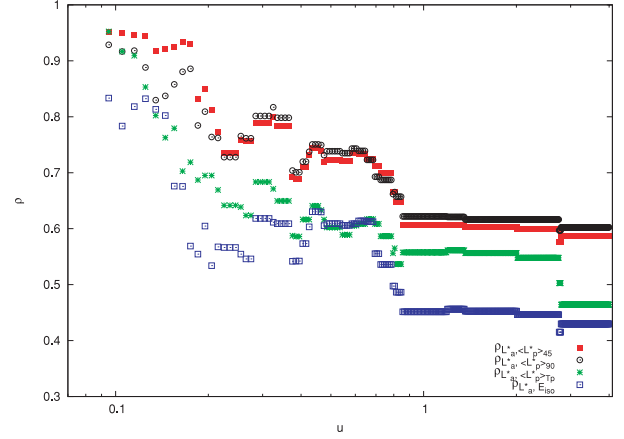


Figure 2. Correlation coefficients ρ for the distributions $\log L_a^* - \log \langle L_p^* \rangle_{45}$ (red squares), $\log L_a^* - \log \langle L_p^* \rangle_{90}$ (black circles), $\log L_a^* - \log \langle L_p^* \rangle_{T_p}$ (green asterisks) and $\log L_a^* - \log E_{\text{iso}}$ (blue squares) for the long GRB subsamples with the varying maximum error parameter u .

Table 2. Spearman correlation coefficients ρ , and the random occurrence probability P , for the listed prompt–afterglow and prompt–prompt distributions (see Table 1 in the online material for the full version of this table). Data for the U4 and U0.095 samples are provided.

Correlation	ρ_{U4}	$\rho_{\text{U0.095}}$	P_{U4}	$P_{\text{U0.095}}$
$L_a^* - \langle L_p^* \rangle_{45}$	0.59	0.95	7.7×10^{-8}	2.3×10^{-3}
$L_a^* - \langle L_p^* \rangle_{90}$	0.60	0.93	7.7×10^{-8}	2.7×10^{-3}
$L_a^* - \langle L_p^* \rangle_{T_p}$	0.46	0.95	2.21×10^{-6}	2.3×10^{-3}
$L_a^* - E_{\text{iso}}$	0.43	0.83	1.4×10^{-5}	3.2×10^{-2}
$T_a^* - E_{\text{iso}}$	-0.19	-0.81	1.0×10^{-1}	5.8×10^{-2}
$L_a^* - E_{\text{peak}}$	0.54	0.74	2.2×10^{-5}	1.7×10^{-2}
$T_a^* - E_{\text{peak}}$	-0.36	-0.74	5.2×10^{-3}	2.5×10^{-2}
$\langle L_p^* \rangle_{45} - E_{\text{peak}}$	0.81	0.76	2.6×10^{-9}	1.2×10^{-3}
$\langle L_p^* \rangle_{45} - E_{\text{iso}}$	0.39	0.42	1.7×10^{-3}	3.0×10^{-1}

with $a = 0.67^{+0.14}_{-0.15}$ and $0.73^{+0.16}_{-0.11}$ for U4 and U0.095 samples, respectively, agreeing with the fit errors. The other distributions considered in this study, involving E_{iso} , $\langle L_p^* \rangle_{90}$, $\langle L_p^* \rangle_{T_p}$ instead of $\langle L_p^* \rangle_{45}$ also show significant correlations, with the lowest u events forming – in all the cases – tightly correlated subsamples of the full distribution (Fig. 2). The resulting correlation coefficients, parameters (a , b) of the fitted correlation lines and the respective probabilities, $P = P(\rho \geq \rho_{\text{pearson}})$ (Bevington & Robinson 2003), generated by chance in a random distribution, are presented in Table 2.

Fig. 2 illustrates the trend in a few tested ‘prompt–afterglow’ distributions to increase the correlation coefficient by selecting the GRBs with the most accurate determination of the plateau-phase parameters, as measured by the error parameter u . The same trend was presented earlier (Dainotti et al. 2010) for the afterglow ($\log L_a^*$, $\log T_a^*$) distribution. In the figure, e.g. we have data derived for 62 long GRBs for $u = 4$, 33 GRBs for $u = 0.3$, 19 GRBs for $u = 0.15$, 13 GRBs for $u = 0.12$ and eight GRBs left for the limiting $u = 0.095$. The prompt emission parameters E_{iso} , $\langle L_p^* \rangle_{90}$ and $\langle L_p^* \rangle_{T_p}$ tested versus the afterglow luminosity L_a^* show significant correlations (cf. Table 2, and its full version in the Supporting Information), but one should note that the mean prompt emission luminosity, $\langle L_p^* \rangle_{45}$, derived using the characteristic time-scale T_{45} , provides the slightly

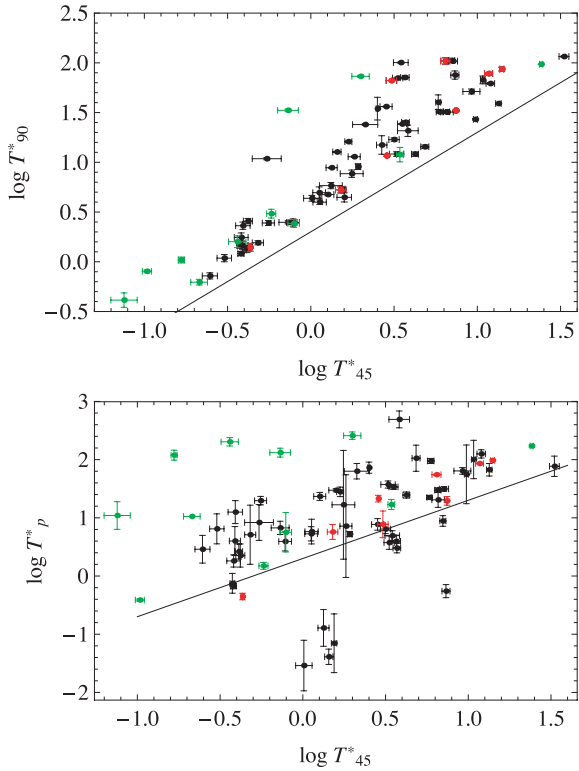


Figure 3. Comparison of the characteristic time-scales for the GRB prompt emission for all the GRBs analysed in this paper. The green points are the IC GRBs, the red ones are the long GRBs with $u \leq 0.095$ and the black ones are the other long GRBs with $u \leq 4$. Upper panel: $\log T_{90}^*$ versus $\log T_{45}^*$ distribution. Lower panel: $\log T_p^*$ versus $\log T_{45}^*$ distribution. The reference lines are $T_{90}^* = 2T_{45}^*$ and $T_{45}^* = T_p^*$ for the upper and lower panels, respectively.

higher value of the Spearman correlation coefficient for small u data points.³ One may also note that the correlations involving the considered mean prompt emission luminosities are higher than the one involving the isotropic energy E_{iso} .

The GRB energy flux of the prompt emission phase is highly non-uniform and distributed non-evenly within the time T_{90} or T_p , as compared to T_{45} (Fig. 3). Thus selecting different characteristic time-scales to derive the mean prompt luminosity is equivalent to considering different physical phases of the prompt emission variation. T_{45} puts a greater emphasis on the peaks of the luminosity, while T_{90} including periods when the emission is low or absent puts therefore more weight on the total elapsed time of the activity period.

Following the above comparison of the considered correlations, we conclude that the presence of tight correlations involving the prompt emission quantities for a small u subsample, defined from the afterglow light curves only, proves that such sample forms a well-defined physical class of standard GRBs with tight relations between their prompt emission and the afterglow light curve properties. Such a tool to extract GRB events enables us to obtain a number of strict relations between their observational parameters, otherwise partly hidden within large scattered samples involving all the available events. In the considered standard GRBs the mechanism causing the prompt phase of the burst influences directly the

³ It is notable that when comparing the times T_{90} and T_{45} , the first one is more dependent on the BAT detector sensitivity limit (Willingale et al. 2010).

afterglow plateau phase, as discussed in literature (Ghisellini et al. 2007; Liang, Zhang & Zhang 2007; Nava et al. 2007; Shao & Dai 2007; Troja et al. 2007; Racusin et al. 2009; Shen et al. 2009).

To better understand how the afterglow plateau phase properties are related to the instantaneous or averaged physical parameters of the prompt emission, we have investigated (see Table 2) the following additional distributions: $E_{\text{iso}}-T_a^*$, $E_{\text{peak}}-L_a^*$, $E_{\text{peak}}-T_a^*$ and $V-L_a^*$. For the $E_{\text{peak}}^*-L_a^*$ distribution we obtain a significant correlation as one could expect from the known $E_{\text{peak}}^*-E_{\text{iso}}^*$ correlation (Amati et al. 2009): $\rho_{L_a^*, E_{\text{peak}}^*} = 0.54$ for the U4 subsample, growing to 0.74 for the U0.095. We have also found a significant $E_{\text{peak}}^*-\langle L_p^* \rangle_{45}$ correlation, shown at the bottom of the Table 2 (for a similar correlation, see Collazzi & Schaefer 2008). Furthermore, since L_a^* is anticorrelated with T_a^* , we derived the expected correlations involving the time-scale T_a^* for the distributions $T_a^*-E_{\text{peak}}^*$ and $T_a^*-E_{\text{iso}}^*$. We note that the correlations involving the time-scale T_a^* are weaker than the ones that correlate the prompt energetic and L_a^* . Instead, for $V-L_a^*$ we did not find any significant correlation or any clear trend for decreasing u subsamples (cf. Ramirez-Ruiz & Fenimore 1999; Lloyd-Romring & Ramirez-Ruiz 2002) for the $V-E_{\text{peak}}$ correlation and analogous relations when these energies are transformed to the source rest frame. If one compares the correlation fit line inclinations, α , given for the U4 and U0.095 (online Table 2) samples, one finds a good agreement – within the error bars – between these samples.

No significant correlations between L_a^* and the prompt emission quantities $\langle L_p^* \rangle_{T_p}$, $\langle L_p^* \rangle_{45}$ and $\langle L_p^* \rangle_{90}$ exist for the $u < 4$ subsample of IC GRB afterglows, including 050724, 051221A, 060614, 060502, 070810, 070809, 070714 (Norris & Bonnell 2010) and 060912A (Levan, Jakobsson & Hurkett 2007), but the number of events is too small to draw any firm conclusion from this fact. Furthermore, for some of these bursts, the determination of the redshift is not so firm, therefore the conclusion of a lack of correlation on this subsample could change with an enlarged and more firm redshift sample.

4 FINAL REMARKS

In this paper we present new significant correlations between the characteristic luminosity of the afterglow plateau phase, L_a^* , and the parameters that characterize the prompt emission, including the mean luminosities and the integral emitted energy. For the afterglow light curves which are well fitted by the Willingale’s phenomenological model, with most accurately determined L_a^* and T_a^* values, we find tight prompt–afterglow correlations in the analysed distributions. Thus, such events can be considered to form the standard GRB sample, to be used both for a detailed physical model discussion for GRB and, possibly, to work out the GRB-related cosmological standard candle. A progress in both issues requires an increase in the number of the well-fitted light curves, not a simple increase of the total number of GRBs with known redshifts.

Correlations between the physical properties of the prompt emission and the luminosity of the afterglow plateau reveal that mean (averaged in time) energetic properties of the prompt emission more directly influence the afterglow plateau phase as compared to E_{iso} , providing new constraints for the physical model of the GRB explosion mechanism. The $(L_a^*, \langle L_p^* \rangle_{45})$ correlation could suggest that the burst and afterglow arise from the same relativistic ejecta, if the energy of those ejecta determined the luminosity of both the prompt and the afterglow phases. Following such an interpretation, we have also studied the correlation between the burst prompt and the afterglow plateau characteristic energies, E_{iso} versus E_a (where $E_a = L_a^* \times T_a$), with a resulting weaker correlation: for U4 sample

of 62 GRBs the Spearman correlation coefficient is 0.39, while for the U0.095 sample of eight GRBs it is 0.42.

No significant prompt–afterglow correlations were detected for the sample of IC GRBs, but the small number of registered events makes it difficult to draw any firm conclusion about the presence or absence of such correlations for the well-fitted IC light-curve shapes.

ACKNOWLEDGMENTS

This work made use of data supplied by the UK Swift Science Data Center at the University of Leicester. MGD and MO are grateful to the Polish Ministry of Science and Higher Education for support through the grant N N203 380336. We thank the anonymous referee for his/her useful comments.

REFERENCES

- Amati L. et al., 2002, *A&A*, 390, 81
 Amati L., Frontera F., Guidorzi C., 2009, *A&A*, 508, 173
 Bevington P. R., Robinson D. K., 2003, *Data Reduction and Error Analysis for the Physical Sciences*, 3rd edn. McGraw-Hill, New York
 Butler N. R., Kocevski D., Bloom J. S., Curtis J. L., 2007, *ApJ*, 671, 656
 Butler N. R., Kocevski D., Bloom J. S., 2009, *ApJ*, 694, 76
 Butler N. R., Bloom J. S., Poznanski D., 2010, *ApJ*, 711, 495
 Cabrera J. I., Firmani C., Avila-Reese V., Ghirlanda G., Ghisellini G., Nava L., 2007, *MNRAS*, 382, 342
 Cannizzo J. K., Gehrels N., 2009, *ApJ*, 700, 1047
 Cannizzo J. K., Troja E., Gehrels N., 2011, *ApJ*, 734, 35C
 Cardone V. F., Capozziello S., Dainotti M. G., 2009, *MNRAS*, 400, 775
 Cardone V. F., Dainotti M. G., Capozziello S., Willingale, 2010, *MNRAS*, 400, 775
 Collazzi A. C., Schaefer B. E., 2008, *ApJ*, 688, 456C
 Cucchiara N. et al., 2011, *ApJ*, 736, 7
 D'Agostini G., 2005, preprint (arXiv:physics/0511182)
 Dainotti M. G., Cardone V. F., Capozziello S., 2008, *MNRAS*, 391, L79
 Dainotti M. G., Willingale R., Capozziello S., Cardone V. F., Ostrowski M., 2010, *ApJ*, 722, L215
 Dainotti M. G., Cardone V. F., Capozziello S., Ostrowski M., Willingale R., 2011, *ApJ*, 730, 135
 Dall'Osso S., Stratta G., Guetta D., Covino S., de Cesare G., Stella L., 2011, *A&A*, 526, 121
 Evans P. et al., 2009, *MNRAS*, 397, 1177
 Fenimore E. E., Ramirez-Ruiz E., 2000, *ApJ*, 539, 712
 Gendre B., Galli A., Piro L., 2007, *A&A*, 465, L13
 Ghirlanda G., Ghisellini G., Lazzati D., 2004, *ApJ*, 616, 331
 Ghirlanda G., Ghisellini G., Firmani C., 2006, *New J. Phys.*, 8, 123
 Ghisellini G., Ghirlanda G., Nava L., Firmani C., 2007, *ApJ*, 658, L75
 Ghisellini G., Nardini M., Ghirlanda G., Celotti A., 2009, *MNRAS*, 393, 253
 Kouveliotou C., Meegan C. A., Fishman G. J., Bhat N. P., Briggs M. S., Koshut T. M., Paciesas W. S., Pendleton G. N., 1993, *ApJ*, 413, L101
 Levan A. J. et al., 2007, *MNRAS*, 378, 1439

- Liang E., Zhang B., 2005, *ApJ*, 633, 611
 Liang E. W., Zhang B., 2006, *MNRAS*, 369, L37
 Liang E. W., Zhang B. B., Zhang B., 2007, *ApJ*, 670, 565
 Lloyd N. M., Petrosian V., 1999, *ApJ*, 511, 550
 Lloyd-Ronning N., Ramirez-Ruiz E., 2002, *ApJ*, 576, 101
 Nava L., Ghisellini G., Ghirlanda G., Cabrera J. I., Firmani C., Avila Reese V., 2007, *MNRAS*, 377, 1464
 Norris J. P., Bonnell J. T., 2006, *ApJ*, 643, 266
 Norris J. P., Bonnell J. T., 2010, *ApJ*, 717, 411
 Norris J. P., Marani G. F., Bonnell J. T., 2000, *ApJ*, 534, 248
 Racusin J. L. et al., 2009, *ApJ*, 698, 43
 Ramirez-Ruiz E., Fenimore E., 1999, *A&A*, 138, 521
 Riechart D. E., Lamb D. Q., Fenimore E. E., Ramirez-Ruiz E., Cline T. L., 2001, *ApJ*, 552, 57
 Sakamoto T., 2008, in Huang Y.-F., Dai Z.-G., Zhang B., eds, *AIP Conf. Proc. Vol. 1065, 2008 Nanjing Gamma-Ray Burst Conference*. Am. Inst. Phys., Melville, p. 9
 Schaefer B. E., 2003, *ApJ*, 583, L67
 Shahmoradi A., Nemiroff R. J., 2009, in Meegan C., Kouveliotou C., Gehrels N., eds, *AIP Conf. Proc. Vol. 1133, Gamma-Ray Burst: Sixth Huntsville Symposium*. Am. Inst. Phys., Melville, p. 425
 Shao L., Dai Z. G., 2007, *ApJ*, 660, 1319
 Shen R.-F., Willingale R., Kumar P., O'Brien P. T., Evans P. A., 2009, *MNRAS*, 393, 598
 Spearman C., 1904, *American J. Psychology*, 15, 72
 Troja E. et al., 2007, *ApJ*, 665, 599
 Willingale R. W. et al., 2007, *ApJ*, 662, 1093
 Willingale R., Genet F., Granot J., O'Brien P. T., 2010, *MNRAS*, 403, 1296
 Xiao L., Schaefer B. E., 2009, *ApJ*, 707, 387
 Yamazaki R., 2009, *ApJ*, 690, L118
 Yonetoku D., Yonetoku D., Murakami T., Nakamura T., Yamazaki R., Inoue A. K., Ioka K., 2004, *ApJ*, 609, 935
 Yu B., Qi S., Lu T., 2009, *ApJ*, 705, L15

SUPPORTING INFORMATION

Additional Supporting Information may be found in the online version of this article:

Table 1. A data list for GRBs with known redshifts analysed in this paper.

Table 2. Spearman correlation coefficients ρ , and the random occurrence probability P , for the listed prompt–afterglow and prompt–prompt distributions.

Please note: Wiley-Blackwell are not responsible for the content or functionality of any supporting materials supplied by the authors. Any queries (other than missing material) should be directed to the corresponding author for the article.

This paper has been typeset from a $\text{\TeX}/\text{\LaTeX}$ file prepared by the author.